Aminoimidazolylmethyluracil Analogues as Potent Inhibitors of Thymidine Phosphorylase and Their Bioreductive Nitroimidazolyl Prodrugs

Philip Reigan,[†] Philip N. Edwards,[†] Abdul Gbaj,[†] Christian Cole,[†] Simon T. Barry,[‡] Ken M. Page,[‡] Susan E. Ashton,[‡] Richard W. A. Luke,[‡] Kenneth T. Douglas,[†] Ian J. Stratford,[†] Mohammed Jaffar,[†] Richard A. Bryce,*[,†] and Sally Freeman*[,†]

School of Pharmacy & Pharmaceutical Sciences, University of Manchester, Oxford Road, Manchester M13 9PL, UK, and AstraZeneca, Alderley Park, Macclesfield, Cheshire SK10 4TG, UK

Received June 25, 2004

Thymidine phosphorylase (TP) is an important target enzyme for cancer chemotherapy because it is expressed at high levels in the hypoxic regions of many tumors and inhibitors of TP have been shown in animal model studies to inhibit angiogenesis and metastasis, and to promote tumor cell apoptosis. The 5-halo-6-[(2′-aminoimidazol-1′-yl)methyl]uracils (**3**, **X** = **Cl**, **Br**) are very potent inhibitors of *E. coli* and human TP with IC_{50} values of ∼20 nM when the enzyme concentration is ∼40 nM. Their 4′-aminoimidazol-1′-yl analogues (**4**, **X** = **Cl**, **Br**) are >350-fold less active with IC_{50} values of ∼7 μM. The 5-unsubstituted analogues (**3 and 4**, **X** = **H**) were both less active than their 5-halo derivatives. Determination of pK_a values and molecular modeling studies of these compounds in the active site of human TP was used to rationalize their activities. The finding that **3**, **X** = **Br** has a poor pharmacokinetic (PK) profile in mice, coupled with the desire for tumor selectivity, led us to design prodrugs. The corresponding 2′-nitroimidazol-1′-ylmethyluracils (**5**, **X** = **Cl**, **Br**) are >1000-fold less active (IC_{50} 22−24 μM) than their 2′-amino analogues and are reduced to the 2′-amino inhibitors (**3**, **X** = **Cl**, **Br**) by xanthine oxidase (XO). As XO is also highly expressed in many tumors, the 2′-nitro prodrugs have the potential to selectively deliver the potent 2′-aminoimidazol-1′-yl TP inhibitors into hypoxic solid tumors.

Introduction

An essential stage in the growth and metastasis of solid tumors is the development of new blood vessels (angiogenesis). Hypoxic tumor cells produce angiogenic growth factors and stimulate the production of these factors in tumor-associated nonmalignant cells. The factor of importance to this study is the cytoplasmic enzyme thymidine phosphorylase (TP, EC 2.4.2.4). TP, which is identical with platelet-derived endothelial cell growth factor (PD-ECGF),[1,2] catalyzes the reversible phosphorolysis of thymidine to thymine and α-D-2-deoxyribose-1-phosphate. A hypothetical transition-state is shown in Scheme 1a.[3,4] The substrates and products are generated by moving the sugar anomeric carbon either toward the thymine nitrogen or toward the phosphate oxygen with only minimal movement of the latter two species. A recent study using arsenate instead of phosphate supports an S_N2-like transition-state for TP.[5]

After it is formed, α-D-2-deoxyribose-1-phosphate is dephosphorylated to 2-D-deoxyribose, which then can be utilized as an oxygen-dependent energy source or it can diffuse (or be transported) out of the cell where it can function as an angiogenic factor (endothelial cell chemoattractant).[6]

Substantially increased expression of TP (up to 10-fold) has been found in many solid tumors relative to surrounding normal tissue.[1−4] Elevated levels of TP are a negative prognostic indicator in breast, ovarian, bladder, pancreatic, gastric, lung, renal, oral/oropharyngeal, oesophageal, liver, uterine endometrial and colorectal cancers, non-Hodgkin's lymphoma, and Kaposi sarcoma and has been associated with invasiveness and malignancy.[1−4] High TP expression in the primary tumor is a risk factor for hepatic metastasis, lymph-node metastasis in gastric carcinoma, and metastasis in invasive breast carcinoma.[7−9] Areas of high blood flow in ovarian and breast tumors show increased TP expression, and this correlates with malignancy.[10,11] In addition, TP confers resistance to apoptosis induced by hypoxia.[12]

Inhibitors of TP may be useful in cancer chemotherapy, as they inhibit angiogenesis and metastasis and promote apoptosis. Until recently, simple monocyclic derivatives of uracil were identified as the best inhibitors of TP, the most quoted being 6-amino-5-bromouracil (**1**, **X** = **Br**) (IC_{50} = 5−30 μM) (Figure 1).[13,14] Its chloro analogue, 6-amino-5-chlorouracil (**1**, **X** = **Cl**), has been reported to block the angiogenic activity of TP.[15] The first purine-based TP inhibitor, 7-deazaxanthine (IC_{50} of 40 μM with *E. coli* TP), has been shown to inhibit angiogenesis in chicken chorioallantoic membranes.[16] A very potent inhibitor of TP, 5-chloro-6-[1-(2′-iminopyrrolidin-1′-yl)methyl]uracil (TPI, **2**) (Figure 1), with a reported IC_{50} value of 35 nM[17] and K_i of 20 nM,[18] has been developed. In addition, Matsushita and co-workers have reported that **2** inhibits the growth of human KB epidermoid carcinoma cells with high TP activity and causes a modest but significant reduction

* Corresponding authors: S.F.: Tel: +44-(0)161-275-2366. Fax: +44-(0)161-275-2396. E-mail: sally.freeman@manchester.ac.uk. R.B. (molecular modeling): Tel: +44-(0)161-275-8345. Fax: +44-(0)161-275-2401. E-mail: richard.bryce@manchester.ac.uk.
† University of Manchester.
‡ AstraZeneca.

10.1021/jm049494r CCC: $30.25
Published on Web 12/24/2004

Scheme 1[a]

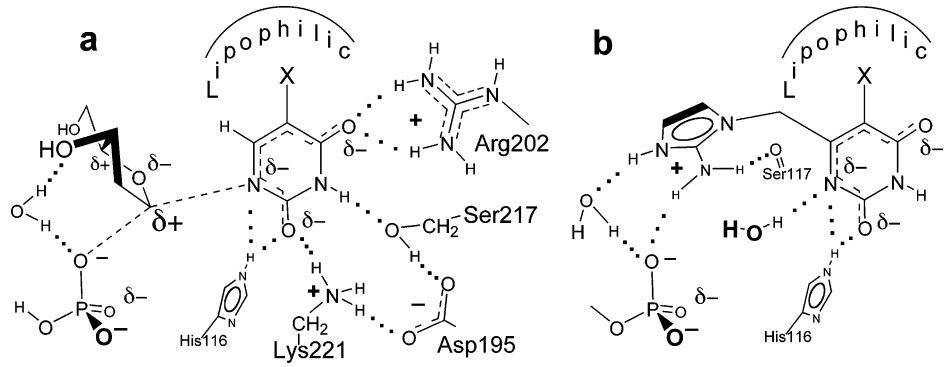

[a] (a) Proposed transition-state in the active site of human TP. (b) 2′-Aminoimidazol-1′-ylmethyluracil (**3, X = Cl**) bound to the active site of TP.

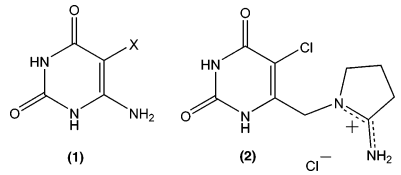

Figure 1. Structures of known TP inhibitors.

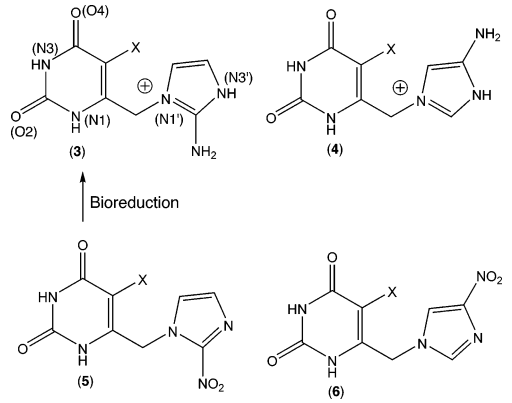

Figure 2. Structures of 2′-/4′-amino- and 2′-/4′-nitro-imidazol-1′-ylmethyluracil analogues. Atom numbers are given for structure (**3**) to aid the molecular modeling discussion.

Scheme 2. Synthesis of 2′/4′-Amino- and 2′/4′-Nitroimidazol-1′-ylmethyluracil Analogues[a]

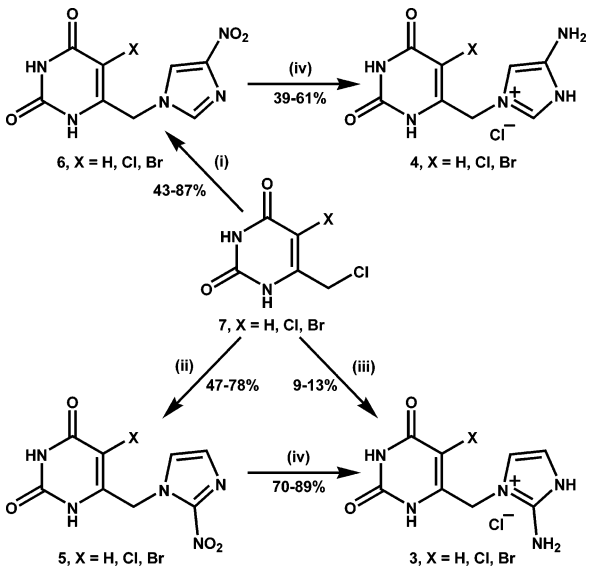

[a] Reagents and conditions (i) 4-nitroimidazole, K_2CO_3 or NaOEt, DMF; (ii) 1-potassio-2-nitroimidazole, DMF; (iii) 2-aminoimidazole sulfate, NaOEt, DMF; (iv) 10% Pd/C, H_2, NH_3, MeOH.

in tumor growth rate when given continuously to mice carrying experimental tumors.[19] Of note, TPI (**2**) in combination with the antitumor agent 2′-deoxy-(5-trifluoromethyl)uridine is currently in phase 1 clinical studies.[20]

Here, we report the design, synthesis, and evaluation of novel aromatic 2′-aminoimidazolyl (**3**) and 4′-aminoimidazolyl (**4**) analogues in which the iminopyrrolidine ring of TPI is replaced with the planar aminoimidazole ring (Figure 2).[21] In addition, their 2′-nitroimidazolyl (**5**) and 4′-nitroimidazolyl (**6**) analogues have been synthesized as potential hypoxia-selective bioreductively activated prodrugs. The identities, locations, and interactions of the active-site groups and water molecules, with substrates and inhibitors, are discussed in the section on modeling.

Results and Discussion

Inhibitor Design and Molecular Modeling. Preliminary molecular modeling studies[21] were completed using a human homology model of TP,[22] which was based on the *E. coli* X-ray crystal structure[23] with which the human form shares 34% sequence homology.[24] This homology model was used to design the 2′- and 4′-aminoimidazolyl analogues **3** and **4**. The imidazole rings of **3**, **X = Cl**, **Br** at the normal intracellular pH of 7.2, were expected to exist largely in their protonated (cationic) forms, while **4** is estimated to be, very approximately, 1% protonated. The cationic groups are expected to interact strongly with *dianionic* monohydrogen phosphate bound to TP in a conformational state that is close to that of the transition-state complex (Scheme 1b). Since the preliminary publication,[21] the X-ray structure of TPI bound to human TP has been published,[25] and here docking of compounds **3**−**6** to the active site of TP has been used to rationalize inhibitory activities (discussed later). The crystals used for the newly available structure do not contain phosphate and indeed no anionic species has been detected in the active site. Clearly, the inclusion of phosphate is essential to any estimates of relative binding energies, so, starting from this closed structure, we have developed a model of the enzyme−substrate complex at the transition-state. Having thereby defined a phosphate-binding locus, we modeled several inhibitors into this more realistic site. The modeling results for the more potent

Table 1. Kinetic Parameters of Thymidine and 5-Nitro-2′-deoxyuridine with *E. coli* and Human TP Using a Continuous Spectrophotometric Assay in 0.1 M Phosphate Buffer pH 7.4 at 25 °C

substrate	enzyme source	$\Delta\epsilon_{kinetics}$, M^{-1} cm^{-1} at $\lambda_{k\ (nm)}$	K_m (mM)	V_{max} (mM/min)	k_{cat} (sec^{-1})	k_{cat}/K_m M^{-1} s^{-1}
thymidine	*E. coli*	2052 at 284	0.24 ± 0.02	1.15 ± 0.044	1770 ± 68	7.4×10^6
5-nitro-2′-deoxyuridine	*E. coli*	7482 at 355	0.23 ± 0.02	0.013 ± 0.0017	20.0 ± 0.6	8.7×10^4
5-nitro-2′-deoxyuridine	human	7482 at 355	0.16 ± 0.03	0.0086 ± 0.0005	2.88	1.8×10^4

compounds discussed in this paper generally are consistent with inhibition data generated with levels of phosphate that should saturate its enzyme binding site(s). However, the modeling powerfully indicates that only a very small subset of known inhibitors is likely to bind preferentially to the spatially restricted, highly organized, closed form of the enzyme.

Chemistry. The 2′-nitro prodrugs were synthesized by coupling the appropriate 5-substituted-6-(chloromethyl)uracil[26] (**7**, **X = H**, **Cl**, **Br**) (Scheme 2) with 1-potassio-2-nitroimidazole to give the 5-substituted-6-[(2′-nitroimidazol-1′-yl)methyl]uracil derivatives (**5**, **X = H**, **Cl**, **Br**) in reasonable yields. In the communication[21] it was reported that reduction of the nitro group in **5** was achieved with $NaBH_4$, whereas our refined method utilizes Pd−C/H_2 to give the desired 6-[(2′-aminoimidazol-1′-yl)methyl]uracil conjugates (**3**, **X = H**, **Cl**, **Br**) in good yields. Alternatively, the 2′-amino derivatives **3** could be synthesized in low yield by direct coupling of the appropriate 5-substituted-6-(chloromethyl)uracil with 2-aminoimidazole. The 4′-nitroimidazolyl prodrugs (**6**, **X = H**, **Cl**, **Br**) were prepared by coupling the appropriate 5-substituted-6-(chloromethyl)uracil (**7**) to 4-nitroimidazole in the presence of either sodium ethoxide or potassium carbonate (Scheme 2). The regioisomeric 5-nitro products were not detected. It should be noted that the synthesis of **6, X = Cl** has very recently been reported (12% yield), along with other 6-methylene-bridged uracil derivatives.[27] The 4′-aminoimidazol-1′-yl analogues (**4**) were prepared by reduction of the 4′-nitro conjugates with Pd−C/H_2. All of the compounds were fully characterized by ^1H and ^{13}C NMR spectroscopy, IR, mass spectrometry, and elemental analysis.

TP Assay. The TP assay was based on the reported continuous assay,[28] in which the synthetic substrate, 5-nitro-2′-deoxyuridine, undergoes phosphorolysis to 5-nitrouracil which, importantly for the UV assay, exists as the N1-anion at the assay pH of 7.4. The assay was modified into a high-throughput, 96-well plate spectrophotometric assay, monitoring an increase in absorbance at 355 nm. The kinetic data for thymidine with *E. coli* TP, and 5-nitro-2′-deoxyuridine with *E. coli* and human TP are given in Table 1. The relative catalytic efficiencies (k_{cat}/K_M) of cleavage of the glycosidic bond of 5-nitro-2′-deoxyuridine by *E. coli* and human TP are similar. For the *E. coli* enzyme, the nitro group in 5-nitro-2′-deoxyuridine decreases the value of k_{cat} by 88-fold compared with thymidine, but has little effect on K_M. The literature values of the K_M for thymidine with TP are 0.38 mM (*E. coli*),[29] 0.187 mM (horse liver),[30] and 0.6 mM (recombinant *E. coli*).[31] The spectral convenience of the nitro substrate is thus accompanied by somewhat decreased sensitivity. TP inhibition kinetics were validated using the inhibitors 6A5BU (**1**, **X = Br**) and TPI (**2**). The data, which are consistent with literature values, are presented in Table 2.

Table 2. Inhibition of *E. coli* TP [pH 7.4, 25 °C, 0.13 mM 5-nitro-2′-deoxyuridine, 45 nM Enzyme] and Human TP (AZ) [pH 7.4, 25 °C, 0.436 mM 5-nitro-2′-deoxyuridine, 0.065 absorbance unit per assay of enzyme] by 2′- and 4′-Amino-6-imidazol-1′-ylmethyluracils (**3**, **4**)[a]

compound	IC_{50} *E. coli*, μM	IC_{50} human (AZ), μM
3, X = H	0.56 ± 0.016	0.1 ± 0.02
3, X = Cl	≤0.0206 ± 0.0014	0.049 ± 0.0013
3, X = Br	≤0.0187 ± 0.0016	0.019 ± 0.002
4, X = H	101.4 ± 1.1	143 ± 20
4, X = Cl	7.3 ± 0.6	26 ± 5.2
4, X = Br	6.50 ± 2	41.0 ± 7.0
TPI	0.02 ± 0.002[b]	0.023 ± 0.005
6A5BU	1.60 ± 0.17	6.8 ± 0.7

[a] Literature IC_{50} values for 6A5BU were 30 μM (horse liver)[13] and 17 μM (recombinant human TP).[32] Literature K_i value of 6A5BU with *E. coli* TP was 0.80 ± 0.12 μM.[33] [b] Measured with an $[E_o]$ of 0.04 μM and represents an upper limit for IC_{50}.[34]

Inhibition of TP by 2′- and 4′-Aminoimidazol-1′-ylmethyluracil Analogues 3 and 4. The 2′- and 4′-aminoimidazol-1′-yl analogues were evaluated for inhibition of recombinant *E. coli* TP. The IC_{50} values in Table 2 show that the 5-halo-6-[(2′-aminoimidazol-1′-yl)methyl]uracils (**3**, **X = Cl**, **Br**) were significantly (>100-fold) more potent than 6A5BU, and, as far as presently can be judged, were as potent as TPI. The relative potencies of **3**, **X = Cl**, **Br** and TPI versus each other and other compounds cannot precisely be judged because these compounds exhibit stoichiometric inhibition at the standard enzyme concentration (the IC_{50} values with *E. coli* TP are indistinguishable from half the enzyme concentration so their K_i values will be >10-fold smaller than the recorded IC_{50} values).[34] The 5-unsubstituted aminoimidazolyl conjugate (**3**, **X = H**) showed a marked decrease in potency compared to the 5-halo conjugates. This is ascribed to the fact that the enzyme residues surrounding the C-5 binding region are highly lipophilic, and in addition the electron-withdrawing effect of the halogen substituent increases the degree of ionization of the uracil N1−H and N3−H (see pK_a section). Also, the greater conformational freedom of **3**, **X = H** in the unbound state, compared to its halogenated analogues, due to the small size of hydrogen, produces an unfavorable entropic contribution to the binding energy. The 4′-aminoimidazolyl analogues (**4**, **X = H**, **Cl**, **Br**) were substantially less active than their 2′-aminoimidazolyl derivatives (**3**, **X = H**, **Cl**, **Br**) (Table 2) due, we suggest, to the small degree of protonation at pH 7.4, the poor ability of the cationic NH group to hydrogen bond directly to the phosphate and the lack of any hydrogen bond to the carbonyl oxygen of Ser117. For TPI and **3**, **X = Br**, the IC_{50} values for *E. coli* TP and human TP were equivalent, but this apparent contrast to some literature reports of species differences may simply reflect our present inability to determine K_i values for these compounds.

Pharmacokinetic (PK) Profile. It was anticipated that the 2′-aminoimidazol-1′-yl analogue (**3**, **X = Br**)

Table 3. Pharmacokinetic Parameters from Mice Dosed with Either TPI or **3**, **X** = **Br** by the ip (10 mg/kg), Oral (20 mg/kg), and iv (2 mg/kg) Routes[a]

compound	dose route	dose (mg/kg)	C_{max} (μg/mL)	T_{max} (h)	AUC (h·μg/mL)	$T_{1/2}$ (h)	F (%)	C_0 (ug/mL)	Cl (mL/min/kg)	V_{dss} (L/kg)
TPI	oral	20	0.391	1	0.990	1.7	52	N/A	N/A	N/A
	ip	10	4.451	5 min	1.658	0.8	>100	N/A	N/A	N/A
	iv	2	N/A	N/A	0.190	0.1	N/A	0.942	>72	2.1
3, X = Br	oral	20	0.350	1	0.968	2.2	33	N/A	N/A	N/A
	ip	10	5.075	5 min	1.505	1.0	103	N/A	N/A	N/A
	iv	2	N/A	N/A	0.292	0.2	N/A	3.751	>72	1.3

[a] Abbreviations: C_{max}, maximum concentration; T_{max}, time to achieve maximum concentration; AUC, area under the curve; $T_{1/2}$, half life; F, bioavailability; C_0, concentration at time 0; Cl, clearance; V_{dss}, volume of distribution at steady state.

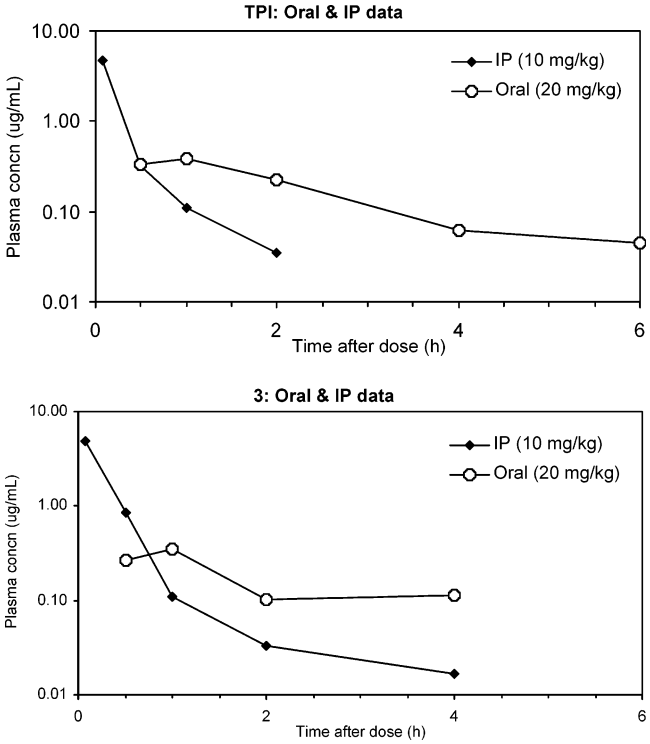

Figure 3. The pharmacokinetic profile of TPI and 6-[(2′-aminoimidazol-1′-yl)methyl]-5-bromouracil (**3**, **X** = **Br**) by intraperitoneal (IP, 10 mg/Kg) and oral (20 mg/Kg) administration.

may passively penetrate cell membranes more readily than TPI (**2**), due to the large difference in basicity of the iminopyrrolidine group compared to the corresponding aminoimidazole group. To test this proposal, a comparative PK study, using TPI and 5-bromo-6-[(2′-aminoimidazol-1′-yl)methyl]uracil (**3**, **X** = **Br**) was undertaken. Mice were dosed with either TPI or **3**, **X** = **Br** by the IP (intraperitoneal), oral, and iv (intravenous) routes at 10, 20, and 2 mg/kg, respectively. Blood samples were taken over a 24 h period following dosing by each route, and corresponding plasma samples were analyzed for TPI or **3**, **X** = **Br** content. PK parameters derived from these data are given in Table 3 and shown in Figure 3. Post-iv clearance was found to be extremely rapid for both compounds (ca. liver blood flow), indicating the likelihood of very low postoral bioavailability, with a correspondingly short $T_{1/2}$. Values for volume of distribution (V_{dss}) were found to be low to moderate, indicating a reasonable degree of tissue penetration. However, the hypothesis that (**3**, **X** = **Br**) would more readily penetrate tissues than TPI due to its less basic character, was confounded by the observation that V_{dss} for the two compounds was similar. It should be noted that plasma levels declined so rapidly following iv administration that these are likely only to be inaccurate estimates of V_{dss}. Following oral administration, the PK profiles of the two compounds were similar, with bioavailability found to be 52 and 33% for TPI and (**3**, **X** = **Br**), respectively. Given the rapid clearance of both compounds following iv doses, this is higher than expected and is likely to be due to saturable elimination or saturable plasma binding, occurring between the iv and oral dose levels. Again, after IP administration, the PK for the two compounds was similar, this time with bioavailability appearing to be complete, although evidence of saturable elimination or binding was also observed on this occasion. Overall, there were few differences in the PK parameters of the two compounds following dosing by the iv, ip, or oral routes; for each, reasonable tissue distribution could be expected, but clearance is so rapid that the duration of any pharmacodynamic effect is unlikely to be prolonged.

Table 4. Inhibition of *E. coli* TP [0.1 M phosphate buffer (pH 7.4), 25 °C, 0.13 mM 5-nitro-2′-deoxyuridine, 45 nM enzyme, measured at 355 nm] and Human TP (AZ) [0.1 M phosphate buffer (pH 7.4), 25 °C, in 0.2 mL total volume containing 0.436 mM 5-nitro-2′-deoxyuridine and TP (0.065 absorbance unit per assay), measured at 355 nm] by 2′/4′-Nitro-6-imidazol-1′-ylmethyluracils (**5**, **6**)

compound	IC_{50} *E. coli*, μM	IC_{50} human (AZ), μM
5, X = H	2.4 ± 0.3	257.7 ± 30
5, X = Cl	21.7 ± 1.2	115 ± 20
5, X = Br	24.4 ± 1.0	160 ± 10
6, X = H	13.8 ± 1.1	500 ± 40
6, X = Cl	7.0 ± 0.8	200 ± 30
6, X = Br	6.60 ± 0.4	181 ± 30

The focus of the next section is concerned with a prodrug approach which, if the prodrug PK properties are favorable, may allow adequate tumor exposure to the 2′-amino imidazol-1′-yl inhibitors produced locally and permit an acceptable dosing schedule.

2′- and 4′-Nitroimidazolyl Prodrugs and Their Bioreduction. Prodrugs containing the nitro group can undergo metabolic reduction, facilitated by bioreductive enzymes, e.g. cytochrome P450-reductase, xanthine oxidase (XO), and low oxygen tension conditions typical of solid tumors.[35–37] A desirable feature in our target prodrug is that it be a poor TP inhibitor. Consistent with this, the 2′-nitro- (**5**) and 4′-nitroimidazol-1′-yl (**6**) analogues showed only weak competitive inhibition of TP (Table 4). Again the 5-unsubstituted uracil analogue was less active than the 5-halo derivatives. For the 5-halo analogues, the 2′-nitro derivatives (**5**, **X** = **Cl**, **Br**) were at least 1000-fold less potent (IC_{50}-nitro/IC_{50}-amino) than the corresponding amino inhibitors (**3**, **X**

Table 5. Kinetic Constants for the Reduction of the 2′-Nitroimidazol-1′-yl Uracil Analogues by XO

compound	ϵ (M^{-1} cm^{-1})	K_m (μM)		V_{max} (ΔA/min)		V_{max} (μM/min)	
		O_2	N_2	O_2	N_2	O_2	N_2
5, X = H	10600	92.4	42.3	0.0057	0.0099	0.535	0.938
5, X = Cl	13800	44.8	25.5	0.0038	0.0106	0.277	0.770
5, X = Br	15200	92.4	23.9	0.0057	0.0109	0.373	0.720

= Cl, **Br**), consistent with the planned use of nitro compounds as prodrugs.

In our recent communication,[21] the proposed bioreduction of the nitro prodrugs to the active amino inhibitors relied on good literature precedence.[35−37] Hypoxia-selective nitroaromatic prodrugs were developed from the early nitroimidazole-based oxygen-mimetic radiosensitizers, such as misonidazole and etanidazole.[38,39] The rates of reduction of many nitroaromatic compounds in an anaerobic XO assay have been documented.[38−41] Here, the 2′-nitroimidazolyl analogues (**5**, **X = H**, **Cl**, **Br**) have been evaluated as reductive prodrug substrates of XO, an enzyme that is overexpressed in many tumors.[42] The nitroreduction reaction was measured by the decrease in extinction at 325 nm, the absorption maxima of the nitro chromophore:[38] neither xanthine nor uric acid show significant absorption at this wavelength. The nitro reductions of the 6-[(2′-nitroimidazol-1′-yl)methyl]uracils (**5**, **X = H**, **Cl**, **Br**) were measured over a concentration range (50−150 μM) under aerobic and anaerobic conditions, and the kinetic data are presented in Table 5. The XO inhibitor allopurinol (10 μM) completely prevented the reduction of the nitroimidazole compounds by XO in both the aerobic and anaerobic assays. The 4′-nitroimidazoyl analogues (**6**, **X = H**, **Cl**, **Br**) were subjected to the same assay, but were extremely poor substrates of XO.

With XO, the 6-[(2′-nitroimidazol-1′-yl)methyl]uracils showed a higher turnover under anaerobic conditions, although nitroreduction was also observed under aerobic conditions. The anaerobic rate constants were comparable to those of other nitroimidazoles reported in the literature.[38,39] Under aerobic conditions, the initial one-electron reduction of the nitro compounds results in the formation of the nitro radical anion, which is redox cycled by molecular oxygen to form the nitro compound (with consequent superoxide ion formation). Under anaerobic conditions redox cycling is minimal and hence turnover is faster. Nitro reduction proceeds through the hydroxylamine derivative, although such compounds are known to be unstable in aqueous solulution (Scheme 3).[43] To confirm the reduction product, the anaerobic reduction of the 5-bromo-6-[(2′-nitroimidazol-1′-yl)-methyl]uracil (**5**, **X = Br**) was repeated. The incubation was prolonged to maximize the final product concentration and the UV spectrum of the product was identical to that of 5-bromo-6-[(2′-aminoimidazol-1′-yl)methyl]-5-halouracil (**3**, **X = Br**). The reaction mixture was filtered using a cellulose-ester filter (0.22 μm pore size) and the filtrate applied to a HPLC Phenomenex C-18 column. The eluted product with the appropriate UV spectrum was confirmed as 5-bromo-6-[1-(2-aminoimidazol-1-yl)-methyl]uracil (**3**, **X = Br**) by NMR analysis.

In summary, the 2′-nitro analogues (**5**, **X = Cl**, **Br**) could be used as hypoxia-mediated bioreductively activated prodrugs of the 2′-aminoimidazolyl inhibitors (**3**, **X = Cl**, **Br**) (Figure 2). Activation will occur in the tumor, where TP and XO are most highly expressed, thus giving additional selectivity to the potential therapy.

Scheme 3. Scheme Showing the Routes of Nitro Reduction of the 2′-Nitroimidazol-1′-ylmethyluracil Analogues under Aerobic (O_2) and Anaerobic (N_2) Conditions[a]

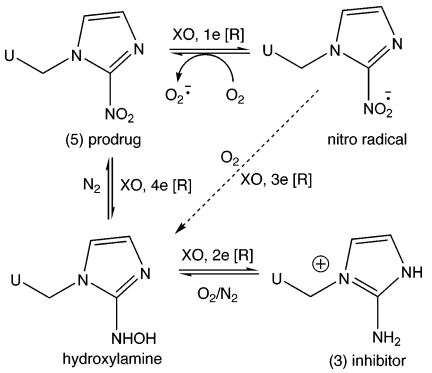

[a] U = appropriate uracil ring.

Rationalization of TP Inhibition. pK_a Measurements. It is has been observed that uracil analogues with a 5-chloro or 5-bromo substituent (**3 or 4**, **X = Cl**, **Br**) are better inhibitors of TP than the unsubstituted derivatives (**3 or 4**, **X = H**) (Table 2). This has also been observed for other classes of TP inhibitors, including TPI (**2**). This may be attributed to the proportion of N(1)−H ionized, at pH 7.4, in the inhibitors and hence their ability to bind to the Arg202 and Lys221 cations (Scheme 1a). The pK_a values of the uracil ring of TPI and the 2′-nitroimidazole analogue (**5**, **X = Br**), measured by UV spectroscopy (300 and 307 nm, respectively) at 25 °C, were 6.14 ± 0.04 and 6.10 ± 0.06, respectively, showing that the 5-halouracil inhibitors are ∼95% ionized at pH 7.4 and ∼22 °C (uracils are ∼2-fold stronger acids at 37 °C than at room temperature). Ionization at both N1−H and N3−H contribute to the observed pK_a but ionization at N-3 will result in very poor binding due to a repulsive interaction between the N3-lone pair and lone pairs on Oγ of Ser217. Making Ser217-OH act as H-bond donor to a N3-lone-pair simply transfers the problem into a repulsion between Ser217Oγ and the carboxylate anion of Asp195 (see Scheme 1a). 5-Halouracils are predicted to ionize predominantly at N3−H since N1−H ionizations are correlated by σ_p-while N3−H are correlated by σ_m, both with ρ-values of 3.4. Estimation of the proportions of ionization at the two nitrogens in the compounds of interest here, using an involved and therefore significantly uncertain process (using Hammett analysis coupled with ΔpK_a values between model compounds), leads to the approximate ratio 2:1 of N1-ionized to N3-ionized, but the uncertainty is ∼3-fold in both directions. The pK_a value of protonated 2-aminoimidazole is 8.5[44] at room temperature (∼8.2 at 37 °C), but the electron-withdrawing effect of the uracil ring will reduce that value in **3**, **X = Cl**, **Br**, **H** by ∼1.2(5-H) to 1.4(5-Hal) units. Substantially smaller effects will apply if the uracil-rings are ionized. These estimates indicate that the 2′-aminoimidazolyl rings of analogues **3, X = Cl**, **Br** are predominantly cationic at pH 7.4 and therefore could interact strongly with

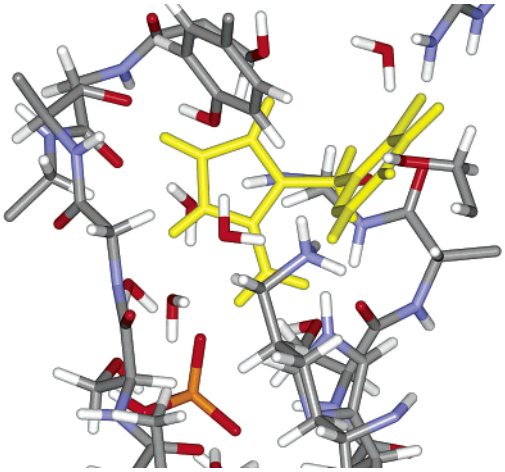

Figure 4. Structure of human TP with bound 6-[(2′-aminoimidazol-1′-yl)methyl]-5-chlorouracil.

phosphate dianion if it is bound in a manner similar to the transition-state complex (Scheme 1b).

In TPI (**2**), the iminopyrrolidine ring will be essentially fully protonated since the pK_a of the protonated form of the close structural analogue 7-methyl-2,3,3a,4,5,6-hexahydro-7H-pyrrolo[2,3-b]pyridine is 11.5.[45] Overall therefore, TPI and the 5-halo-6-[(2′-aminoimidazol-1′-yl)methyl]uracils (**3**, **X = Cl**, **Br**) are expected to be zwitterionic at pH 7.4. In contrast, since uracil has a pK_a of 9.43[46] (with both N−H groups contributing to the observed value), the situation for **3**, **X = H** is more complex, all four species (zwitterionic, neutral, anionic and cationic) are likely to coexist in significant amounts (especially at 37 °C), and the estimation of their proportions is uncertain (even discounting ionization at 'uracil'−N3, four micro pK_a values would be required); however, the proportion of the *required* zwitterion is likely to be small and binding to HPO_4^{2-} and cationic Arg202 and Lys221 at the active site will be compromised (to save space, Arg202 and Lys221 are not shown in Scheme 1b).

Molecular Modeling with Human TP. Based on the recent crystal structure,[25] a molecular model of the closed form of human TP was constructed, with addition of a dianionic phosphate group in the active site. Subsequently, complexes of TP with the zwitterionic forms of 2′-aminoimidazoyluracil inhibitors **3** and TPI, and its bromo and nonhalogenated analogues were modeled into the active site. The N1-anionic uracil moieties of the inhibitors form hydrogen bonds with Arg202, Ser217, Lys221, and His116, as expected (Figure 4). The iminopyrrolidine and aminoimidazole rings bind perpendicularly to the plane of the uracil ring, with the planar NH_2 groups binding tightly through one H to phosphate and through the other to the carbonyl oxygen of Ser117 (Figure 4). There are only minor differences in the binding geometry of the puckered pyrrolidines and the planar imidazoles. A water molecule occupies space around and beyond the region where the sugar-C2′ would fit. We note that the ring-NH in the 2-aminoimidazolium types is forced to share the oxygen of a water molecule otherwise exclusively involved in bonding to the amidic-NH of Thr154. All the modeled inhibitors exhibit a high degree of steric complementarity to the active site; substitution at any position by a group larger than that present is predicted to be deleterious.

Table 6. Calculated Inhibitor−TP Binding Energies and Components (kcal/mol)

compound	ΔE_{int}^{elec}	ΔE_{int}^{vdw}	ΔE_{int}	ΔG_{solv}^{elec}	ΔG_{solv}	ΔE_{bind}^{elec}	ΔE_{bind}
TPI (X = Cl)	0.3	−0.3	0.0	−44.7	−40.4	1.1	0.8
TPI (X = Br)	0.0	0.0	0.0	−43.9	−39.5	0.0	0.0
TPI (X = H)	−2.0	1.7	−0.3	−49.1	−46.1	3.2	6.3
3, X = Cl	−8.1	2.6	−5.6	−48.5	−43.2	−3.5	−1.8
3, X = Br	−8.5	2.6	−5.9	−47.5	−42.3	−4.9	−3.0
3, X = H	−10.9	4.6	−6.4	−53.3	−49.3	−1.6	3.4

The faces of the uracil rings contact lipophilic residues over most of their surface area and similar contacts continue over most of the surface of uracil-C5 substituents larger than hydrogen: the site designed for the methyl group of thymine, composed of residues Thr118, Leu148, Val208, Ile214, and Val241, readily accommodates chloro or bromo analogues (Figure 4).

For both the modeled 2′-aminoimidazoyluracil and TPI sets, calculated interaction energies (ΔE_{int}) do not strongly discriminate between bromo, chloro, and nonhalogenated compounds (Table 6). However, a more favorable van der Waals interaction is observed for the halogenated ligands, consistent with improved interaction at the lipophillic pocket with the larger C5 substituent size. Interestingly, the 2′-aminoimidazoyluracils are predicted to interact more favorably than the TPI derivatives by 5.8 kcal/mol on average (Table 6). The calculated preferential interaction of the 2′-aminoimidazoyluracils is electrostatic in nature and may be related to improved polar interactions with TP associated with the additional NH-group in the five-membered aminoimidazole ring. The ligand NH donates a hydrogen bond to a water molecule that bridges with the backbone HN of Thr154, the Oγ of Ser144, and a phosphate oxygen (Figure 4).

Inclusion of ligand desolvation in relative binding energies (ΔE_{bind}) leads to ranking of compounds Br > Cl > H (Table 6) for both 2′-aminoimidazoyluracil and TPI sets, in accord with IC_{50} values for *E. coli* TP (Table 2). Discrimination by TP against the nonhalogenated compounds at C5 arises from strong differential solvation of the nonhalogenated ligands in aqueous solution as predicted by the COSMO solvent model.[47,48] The larger halogen atoms partially occlude solvent interactions with the adjacent NH_2 group of the five-membered ring. Overall, therefore, calculations predict preference of halogen over H at C5 in both **3** and TPIs, due to combined contributions of improved filling of a lipophilic pocket by the halogen atom and larger desolvation penalty due to the H atom. We also note that the 2′-aminoimidazoyluracil compounds are preferentially solvated over the corresponding TPI analogues by a mean value of 3.0 kcal/mol (Table 6). Again, this may be due to the presence of the additional heteroatom in the five-membered imidazole ring. Consequently, the overall preference of TP for 2′-aminoimidazoyluracil over TPI-type compounds is reduced. It is unclear from IC_{50} measurements with TP as to which inhibitor type is preferred (Table 2), due to the tight binding nature of the compounds at the enzyme concentrations employed.

By contrast, the 2-nitroimidazole analogue of TPI (**5**), modeled as an anion rather than a zwitterion and with the NO_2 group distal from phosphate, has a large

positive calculated relative interaction energy (>100 kcal/mol), suggesting that one must consider the possibility that the $\sim 10^{-8}$ % of zwitterionic 2-nitroimidazole compound at pH 7.4 is the species that actually binds. This fraction is estimated from a pK_a of −0.48 for 1-methyl-2-nitroimidazolium cation.[49] However, calculations indicate the zwitterionic form of the 4-aminoimidazole compound is, relative to TPI, very poorly bound, suggesting that the nitro compound binds to an alternative, presumably more open conformer of TP and perhaps to a complex that lacks dianionic phosphate.

Conclusion

A computational modeling study of the aminoimidazolyl compounds (**3**) based on the recent X-ray structure of human TP confirmed that their binding was energetically more favored than that of their corresponding nitro counterparts. This has been confirmed with inhibition studies for both *E. coli* and human TP. 5-Bromo-6-[(2′-aminoimidazol-1′-yl)methyl]uracil ($IC_{50} < 19 \pm 2$ nM for *E. coli* TP and $IC_{50} = 22 \pm 3$ nM for human TP) is a tight-binding potent TP inhibitor; however, its PK properties are poor. For the 5-halo-2′-aminoimidazoyl compounds (**3**, **X** = **Cl**, **Br**) there is at least a 1000-fold increase in potency in TP inhibition compared with the nitro prodrugs (**5**, **X** = **Cl**, **Br**). The nitro compounds are reduced by XO to the amino TP inhibitors. Therefore, this approach can potentially be used to deliver very potent TP inhibitors preferentially into hypoxic solid tumors.

Experimental Section

Chemicals and biochemicals were obtained from the Sigma-Aldrich Chemical Co. Dorset, UK. and Lancaster Synthesis Ltd. Lancashire, UK. Adsorber resin Amberlite XAD-4 20−50 mesh for column chromatography was obtained from BDH, VWR International, Leicestershire, UK. Deuterated solvents (DMSO-d_6, D_2O, and $CDCl_3$) and tetramethylsilane (TMS) were supplied by Cambridge Isotope Laboratories Inc. Andover, MA.

5-Nitro-2′-deoxyuridine was prepared according to a literature procedure[50] as colorless crystals, mp 149−151 °C (lit. mp[51] 149−150 °C). TPI (**2**),[17] and 6A5BU (**1**, **X** = **Br**)[14] were synthesized using literature methods. 5-Chloro-6-(chloromethyl)uracil or 5-bromo-6-(chloromethyl)uracil were prepared from 6-(chloromethyl)uracil with NCS or NBS, respectively.[26]

The enzymes xanthine oxidase (X4376, 0.4 unit/mg protein, one unit will convert 1.0 μmol of xanthine to uric acid per minute at pH 7.5 at 25 °C) from buttermilk, recombinant *E. coli* thymidine phosphorylase (T2807, 1060 units/mL, one unit will convert 1.0 μmol each of thymidine and phosphate to thymine and 2-deoxyribose-1-phosphate per minute at pH 7.4 at 25 °C) and recombinant human thymidine phosphorylase (T9319, 9−10 unit/mg protein, one unit will form 1 nmol thymine per minute at pH 7.0 at 37 °C), expressed in V79 Chinese hamster cells.

Analytical Instrumentation. Analytical thin-layer chromatography (TLC) was performed on Merck precoated silica gel 60 F_{254} plates and visualized by ultraviolet (UV) illumination (254 nm) using a UV GL-58 mineral-light lamp or by staining with $KMnO_4$ or I_2. Melting points (mp) were determined either in open glass capillary tubes on Gallenkamp M.P.D.350.BM2.5 micro melting point apparatus or on a Köfler melting point microscope and are uncorrected. Nuclear magnetic resonance (NMR) spectra were recorded on a 300 MHz Bruker Avance 300 spectrometer using X-win NMR software, operating at 300 MHz for ^{1}H NMR spectra and 68 MHz for ^{13}C NMR spectra. ^{1}H NMR spectra were recorded in δ_H parts per million (ppm) in DMSO-d_6 or $CDCl_3$ with TMS as an internal standard or in D_2O with benzene as reference. Data are reported using the following convention: chemical shift (integrated intensity, splitting pattern, coupling constant, assignment). The following abbreviations are used: s = singlet, d = doublet, dd = double doublet, t = triplet, quart = quartet, quint = quintet, sext = sextet, m = multiplet and br = broad. The coupling constants (J) are expressed in Hertz (Hz). ^{13}C NMR spectra were recorded in δ_C parts per million (ppm) in DMSO-d_6 or $CDCl_3$ with TMS and the solvent peak as internal standards. ^{13}C DEPT-135 NMR spectra confirmed assignment.

Infrared (IR) spectra were recorded on a Satellite FTIR Mattson spectrometer, with Mattson WinFIRST software. The samples were prepared on a Specac golden gate single reflection ATI system. High performance liquid chromatography (HPLC) analysis was performed on an Agilent HPLC 1100 Series with ChemStation software, using a Phenomenex C-18 analytical column with a security guard attachment. Mass spectra (MS) and elemental analysis were determined at the Department of Chemistry, University of Manchester. Electron ionization (EI) and positive and negative chemical ionization (CI) mass spectra were recorded from an automated Fisons TRIO 2000 quadrapole spectrometer. Both positive and negative electrospray (ES) ionization and atmospheric pressure chemical ionization (APCI) mass spectra were recorded using a Micromass Platform II atmospheric pressure ionization spectrometer coupled to an HPLC system, used for the analysis of nonvolatile and thermally labile materials directly from solution.

Water was distilled and purified by ion exchange and charcoal using a MilliQ system (Millipore Ltd). Values of pH were measured using a Hanna-instruments HI 9321 microprocessor pH meter, calibrated with standard buffers at 20 °C. TP rate assays, spectral scans and absorbance readings at fixed wavelengths were conducted spectrophotometrically using a Peltier-thermostated cuvette holder in a Cary 1E UV−visible spectrophotometer and the Cary Enzyme Kinetics Software. A thermostated 96-well Molecular Devices (Spectramax) spectrophotometer was used. Quartz cuvettes were used in the UV range and for determining extinction coefficients. Enzyme kinetics and other data were analyzed using Grafit software Version 3 (Erithacus, supplied by Sigma Chemicals Co.Ltd). For XO enzyme kinetics, UV spectra were recorded on a Unicam UV 300 spectrophotometer, with Thermospectronic Vision 32 software, using Hellma UV quartz cuvettes.

The pK_a values of inhibitors were determined spectrophotometrically on the Cary instrument at 25 °C using acetate, HEPES, phosphate and Tris buffers at 0.1 M.

6-[(2′-Nitroimidazol-1′-yl)methyl]uracil (5, X = H). A mixture of 6-(chloromethyl)uracil (0.32 g, 2.0 mmol, 1 equiv) and 1-potassio-2-nitroimidazole salt (0.54 g, 3.6 mmol, 1.8 equiv) was stirred in anhydrous DMF (4.0 mL) at 75 °C under a N_2 atmosphere for 2 h. The reaction mixture was diluted with water (15 mL), and the precipitate was removed by filtration and then stirred in hot water (5 mL), filtered and vacuum-dried to yield **5** (**X** = **H**) as a pale-brown powder (0.28 g, 60%). Mp >320 °C. ^{1}H NMR (DMSO-d_6): δ_H 5.00 (1H, s, C5−H), 5.34 (2H, s, CH_2), 7.28 (1H, d, $^3J_{HH}$ = 1.0 Hz, C4′-H), 7.73 (1H, d, $^3J_{HH}$ = 1.0 Hz, C5′-H), 11.14 (1H, s, NH), 11.27 (1H, s, NH). ^{13}C NMR (DMSO-d_6): δ_C 48.3 (CH_2), 96.8 (C-5), 128.0 (C-4′), 128.1 (C-5′), 144.5 (C-2′), 151.1 (C-2), 151.2 (C-6), 163.5 (C-4). MS-ESI *m/z* 236 (M − H, 100%). Anal. ($C_8H_7N_5O_4$) C, H, N.

5-Chloro-6-[(2′-nitroimidazol-1′-yl)methyl]uracil (5, X = Cl). A mixture of 5-chloro-6-(chloromethyl)uracil (0.29 g, 1.5 mmol, 1 equiv) and 1-potassio-2-nitroimidazole salt (0.45 g, 3.0 mmol, 2 equiv) was stirred in anhydrous DMF (7.0 mL) at room temperature under an N_2 atmosphere for 24 h. The reaction mixture was diluted with water (15 mL) and the precipitate removed by filtration, acidified with aqueous 1.0 M HCl, and cooled at 5 °C until a precipitate formed. This precipitate was isolated by filtration, washed with methanol, and vacuum-dried to yield **5** (**X** = **Cl**) as a beige powder (0.14 g, 47%). Mp >320 °C. ^{1}H NMR (DMSO-d_6): δ_H 5.56 (2H, s,

CH_2), 7.23 (1H, d, $^3J_{HH}$ = 1.1 Hz, C4′-H), 7.68 (1H, d, $^3J_{HH}$ = 1.1 Hz, C5′-H), 11.36 (1H, s, NH), 11.71 (1H, s, NH). ^{13}C NMR (DMSO-d_6): δ_C 47.5 (CH_2), 106.3 (C-5), 127.3 (C-4′), 128.1 (C-5′), 144.7 (C-6), 145.2 (C-2′), 149.8 (C-2), 159.6 (C-4). MS-ESI *m/z* 270 (^{35}Cl M−H, 90%), 272 (^{37}Cl M − H, 30%). Anal. ($C_8H_6ClN_5O_4$) C, H, N.

5-Bromo-6-[(2′-nitroimidazol-1′-yl)methyl]uracil (5, X = Br). 5-Bromo-6-(chloromethyl)uracil (0.25 g, 1.0 mmol, 1 equiv) and 1-potassio-2-nitroimidazole salt (0.31 g, 2.0 mmol, 2 equiv) were stirred in anhydrous DMF (3.0 mL) at room temperature under a N_2 atmosphere. After 23 h the fully dissolved reaction mixture was diluted with water (10 mL) and a precipitate slowly formed, which was removed by filtration. The filtrate was acidified with aqueous 1.0 M HCl and cooled at 5 °C until a precipitate formed. This precipitate was isolated by filtration, washed with methanol and vacuum-dried to yield **5** (**X = Br**) as a beige powder (0.25 g, 78%). Mp >320 °C. ^{1}H NMR (DMSO-d_6): δ_H 5.53 (2H, s, CH_2), 7.23 (1H, d, $^3J_{HH}$ = 1.1 Hz, C4′-H), 7.66 (1H, d, $^3J_{HH}$ = 1.1 Hz, C5′-H), 11.36 (1H, s, NH), 11.69 (1H, s, NH). ^{13}C NMR (DMSO-d_6): δ_C 49.7 (CH_2), 96.7 (C-5), 127.1 (C-4′), 128.1 (C-5′), 145.2 (C-2′), 146.5 (C-6), 150.2 (C-2), 159.8 (C-4). MS-ESI *m/z* 313 (^{79}Br M − H, 100%), 315 (^{81}Br M − H, 85%). Anal. ($C_8H_6BrN_5O_4$) C, H, N.

6-[(4′-Nitroimidazol-1′-yl)methyl]uracil (6, X = H). A mixture of 6-(chloromethyl)uracil (0.47 g, 2.9 mmol, 1 equiv), 4-nitroimidazole (0.65 g, 5.8 mmol, 2 equiv), and K_2CO_3 (0.83 g, 6.0 mmol, 2.1 equiv) was stirred in anhydrous DMF (1.0 mL) at room temperature under a N_2 atmosphere. After 23 h, water (14 mL) was added to the red mixture and the precipitate removed by filtration. The filtrate was then acidified with aqueous 1.0 M HCl, and the crude product was isolated by filtration as a pale-red powder. The powder was dissolved in aqueous 1.0M NaOH, decolorized with charcoal, filtered through Celite, and then acidified with aqueous 1.0M HCl. The title compound (**6**, **X = H**) was isolated by filtration as an off-white powder (0.33 g, 70%). Mp >320 °C. ^{1}H NMR (DMSO-d_6): δ_H 5.05 (2H, s, CH_2), 5.20 (1H, s, C5−H), 7.94 (1H, d, $^4J_{HH}$ = 1.4 Hz, C5′-H), 8.45 (1H, d, $^4J_{HH}$ = 1.4 Hz, C2′-H), 11.06 (1H, s, NH), 11.20 (1H, s, NH). ^{13}C NMR (DMSO-d_6): δ_C 46.9 (CH_2), 98.8 (C-5), 121.9 (C-5′), 137.8 (C-2′), 147.1 (C-4′), 150.3 (C-6), 151.2 (C-2), 163.7 (C-4). MS-ESI *m/z* 236 (M − H, 100%). Anal. ($C_8H_7N_5O_4 \cdot H_2O$) C, H, N.

5-Chloro-6-[(4′-nitroimidazol-1′-yl)methyl]uracil (6, X = Cl). A mixture of 5-chloro-6-(chloromethyl)uracil (0.20 g, 1.0 mmol, 1 equiv), 4-nitroimidazole (0.24 g, 2.0 mmol, 2 equiv), and NaOEt (0.14 g, 2.0 mmol, 2 equiv) was stirred in anhydrous DMF (1.0 mL) at 80 °C under an N_2 atmosphere. After 3 h, the reaction was allowed to cool. The reaction mixture was diluted with water (7 mL) and the precipitate removed by filtration. The filtrate was acidified with aqueous 1.0M HCl and cooled at 5 °C until a precipitate formed. The title compound (**6**, **X = Cl**) was isolated by filtration as a beige powder (0.24 g, 87%). Mp >320 °C. ^{1}H NMR (DMSO-d_6): δ_H 5.19 (2H, s, CH_2), 7.95 (1H, d, $^4J_{HH}$ = 1.4 Hz, C5′-H), 8.43 (1H, d, $^4J_{HH}$ = 1.4 Hz, C2′-H), 11.51 (1H, s, NH), 11.70 (1H, s, NH). ^{13}C NMR (DMSO-d_6): δ_C 46.2 (CH_2), 107.8 (C-5), 122.0 (C-5′), 138.2 (C-2′), 144.6 (C-6), 147.4 (C-4′), 150.3 (C-2), 160.2 (C-4). MS-ESI *m/z* 270 (^{35}Cl M − H, 90%), 272 (^{37}Cl M − H, 30%). Anal. ($C_8H_6ClN_5O_4$) C, H, N.

5-Bromo-6-[(4′-nitroimidazol-1′-yl)methyl]uracil (6, X = Br). A mixture of 5-bromo-6-(chloromethyl)uracil (0.24 g, 1.0 mmol, 1 equiv), 4-nitroimidazole (0.24 g, 2.1 mmol, 2.1 equiv), and NaOEt (0.15 g, 2.2 mmol, 2.2 equiv) was stirred in anhydrous DMF (1.0 mL) at 80 °C under an N_2 atmosphere. After 1 h, the reaction was allowed to cool. The reaction mixture was diluted with water (5 mL) and the precipitate removed by filtration. The filtrate was acidified with aqueous 1.0 M HCl and was cooled at 5 °C until a precipitate formed. The title compound (**6**, **X = Br**) was isolated by filtration as an orange powder (0.14 g, 43%). Mp 287.5−288 °C. ^{1}H NMR (DMSO-d_6): δ_H 5.18 (2H, s, CH_2), 7.99 (1H, d,$^4J_{HH}$ = 1.4 Hz, C5′-H), 8.43 (1H, d, $^4J_{HH}$ = 1.4 Hz, C2′-H), 11.66 (1H, s, NH), 11.83 (1H, s, NH). ^{13}C NMR (DMSO-d_6): δ_C 48.5 (CH_2), 98.5 (C-5), 121.9 (C-5′), 138.1 (C-2′), 146.3 (C-6), 147.4 (C-4′), 150.6 (C-2), 160.5 (C-4). MS-ESI *m/z* 313 (^{79}Br M − H, 50%), 315 (^{81}Br M − H, 50%). Anal. ($C_8H_6BrN_5O_4$) C, H, N.

6-[(2′-Aminoimidazol-1′-yl)methyl]uracil Hydrochloride (3, X = H). A mixture of 6-[(2′-nitroimidazol-1′-yl)methyl]-uracil (0.19 g, 0.8 mmol, 1 equiv) in methanol (20 mL) containing concentrated aqueous NH_3 (0.50 mL, 6.6 mmol, 8.25 equiv) and 10% Pd/C (40 mg) was stirred in a H_2 atmosphere at room temperature for 5 h. The catalyst was removed by filtration through Celite and the solvent evaporated. The residue was dissolved in aqueous 0.1 M HCl (20 mL) and evaporated to dryness, giving **3, X = H** as a beige powder (0.17 g, 88.5%). Mp 296.5−298 °C. ^{1}H NMR (DMSO-d_6): δ_H 4.87 (1H, s, C5−H), 4.93 (1H, s, CH_2), 5.54 (1H, d, $^3J_{HH}$ = 2.3 Hz, C5′-H), 6.99 (1H, d, $^3J_{HH}$ = 2.3 Hz, C4′-H), 8.03 (2H, s, $-NH_2$), 11.06 (1H, s, NH), 11.33 (1H, s, NH), 12.35 (1H, s, NH). ^{13}C NMR (DMSO-d_6): δ_C 44.2 (CH_2), 96.9 (C-5), 113.2 (C-4′), 116.3 (C-5′), 146.8 (C-2′), 150.3 (C-6), 151.1 (C-2), 163.6 (C-4). MS-ESI *m/z* 209 (M^+, 100%). MS-AP *m/z* 209 (M^+, 100%). Anal. ($C_8H_{10}ClN_5O_2$) C, H, N.

6-[(2′-Aminoimidazol-1′-yl)methyl]-5-chlorouracil Hydrochloride (3, X = Cl). Procedure A. A mixture of 5-chloro-6-(chloromethyl)uracil (0.38 g, 2.0 mmol, 1 equiv), 2-aminoimidazole sulfate (0.51 g, 3.9 mmol, 1.9 equiv), and NaOEt (0.28 g, 4.1 mmol, 2.1 equiv) was stirred in anhydrous DMF (2.0 mL) at room temperature under an N_2 atmosphere for 26 h. The reaction mixture was filtered and the solid added to water (3.0 mL), which was neutralized with glacial AcOH. The insoluble material was collected by filtration, dissolved in aqueous 0.1 M HCl (17 mL), decolorized with activated charcoal, and removed by filtration through Celite, and the filtrate was evaporated to dryness. The resulting solid was washed with a minimum of ethanol and filtered to yield **3, X = Cl** as a pale-yellow powder (0.07 g, 13%).

Procedure B. A mixture of 5-chloro-6-[(2′-nitroimidazol-1′-yl)methyl]uracil (**5**, **X = Cl**) (0.22 g, 0.8 mmol, 1 equiv) in methanol (20 mL) containing concentrated aqueous NH_3 (0.5 mL, 6.6 mmol, 8.25 equiv) and 10% Pd/C (40 mg) was stirred in a H_2 atmosphere at room temperature for 3 h. The catalyst was removed by filtration through Celite and the solvent evaporated. The residue was dissolved in aqueous 0.1 M HCl (20 mL) and evaporated to dryness, giving **3, X = Cl** as a beige powder (0.18 g, 82%). Mp >320 °C. ^{1}H NMR (DMSO-d_6): δ_H 5.06 (2H, s, CH_2), 6.97 (1H, d, $^3J_{HH}$ = 2.6 Hz, C4′-H), 6.99 (1H, d, $^3J_{HH}$ = 2.6 Hz, C5′-H), 8.00 (2H, s, $-NH_2$), 11.59 (1H, s, NH), 11.73 (1H, s, NH), 12.29 (1H, s, NH). ^{13}C NMR (DMSO-d_6): δ_C 43.4 (CH_2), 106.4 (C-5), 113.4 (C-4′), 115.4 (C-5′), 144.6 (C-6), 147.2 (C-2′), 149.7 (C-2), 159.6 (C-4). MS-ESI *m/z* 242 (^{35}Cl M^+, 100%), 244 (^{37}Cl M^+, 30%). MS-AP *m/z* 242 (^{35}Cl M^+, 100%). Anal. ($C_8H_9Cl_2N_5O_2$) C, H, N.

6-[(2′-Aminoimidazol-1′-yl)methyl]-5-bromouracil Hydrochloride (3, X = Br). Procedure A. A mixture of 5-bromo-6-(chloromethyl)uracil (0.29 g, 1.5 mmol, 1 equiv), 2-aminoimidazole sulfate (0.39 g, 2.9 mmol, 2 equiv), and NaOEt (0.21 g, 3.0 mmol, 2 equiv) was stirred in anhydrous DMF (1.0 mL) at room temperature under an N_2 atmosphere for 25 h. The reaction mixture was then diluted with DMF (1 mL) and filtered and the solid added to water (3.0 mL), which was neutralized with glacial AcOH. The insoluble material was collected by filtration, dissolved in aqueous 0.1 M HCl (6.0 mL), and evaporated to dryness. The solid was then dissolved in water (8 mL), decolorized with activated charcoal, and removed by filtration through Celite and the filtrate evaporated to dryness. The remaining solid was washed with a minimum of ethanol and filtered to yield **3, X = Br** as a cream powder (0.04 g, 9%).

Procedure B. A mixture of 6-[(2′-nitroimidazol-1′-yl)-methyl]-5-bromouracil (**5**, **X = Br**) (0.25 g, 0.8 mmol, 1 equiv) in methanol (20 mL) containing concentrated aqueous NH_3 (0.5 mL, 6.6 mmol, 8.25 equiv) and 10% Pd/C (40 mg) was stirred in a H_2 atmosphere at room temperature for 5 h. The catalyst was removed by filtration through Celite and the solvent evaporated. The residue was dissolved in aqueous 0.1 M HCl (20 mL) and evaporated to dryness, to give **3, X = Br** as a beige powder (0.18 g, 70%). Mp 289−289.5 °C. ^{1}H NMR

(DMSO-d_6): δ_H 5.01 (2H, s, CH_2), 6.97 (2H, s, C5′-H and C4′-H), 7.98 (2H, s, $-NH_2$), 11.61 (1H, s, NH), 11.71 (1H, s, NH), 12.27 (1H, s, NH). ^{13}C NMR (DMSO-d_6): δ_C 46.3 (CH_2), 96.9 (C-5), 113.3 (C-4′), 115.3 (C-5′), 146.2 (C-6), 147.2 (C-2′), 150.1 (C-2), 159.8 (C-4). MS-ESI *m/z* 286 (^{79}Br M$^+$, 100%), 288 (^{81}Br M$^+$, 95%). MS-AP *m/z* 286 (^{79}Br M$^+$, 100%), 288 (^{81}Br M$^+$, 97%). Anal. ($C_8H_9BrClN_5O_2$) C, H, N.

6-[(4′-Aminoimidazol-1′-yl)methyl]uracil Hydrochloride (4, X = H). A mixture of 6-[(2′-nitroimidazol-1-yl)methyl]-uracil (0.19 g, 0.8 mmol, 1 equiv) in methanol (20 mL) containing concentrated aqueous NH_3 (0.5 mL, 6.6 mmol, 8.25 equiv) and 10% Pd/C (40 mg) was stirred in a H_2 atmosphere at room temperature for 5 h. The catalyst was removed by filtration through Celite and the solvent evaporated. The residue was dissolved in a minimum of water and chromatographed on an Amberlite XAD-4 resin column (4:1, v/v, H_2O/MeOH). The major fraction was isolated and evaporated to dryness giving a brown residue. The residue was dissolved in aqueous 0.1 M HCl (20 mL) and evaporated to dryness, to give **4, X = H** as a red/brown powder (0.12 g, 61%). Mp 295−296 °C. ^{1}H NMR (DMSO-d_6): δ_H 4.94 (2H, s, CH_2), 5.16 (1H, s, C5−H), 6.99 (1H, d, $^4J_{HH}$ = 1.2 Hz, C5′-H), 7.07 (1H, d, $^4J_{HH}$ = 1.2 Hz, C2′-H), 8.03 (2H,s, $-NH_2$), 11.13 (1H, s, NH), 11.32 (1H, s, NH), 12.36 (1H, s, NH). ^{13}C NMR (DMSO-d_6): δ_C 44.2 (CH_2), 96.9 (C-5), 123.2 (C-4′), 126.3 (C-5′), 144.1 (C-2′), 146.8 (C-6), 150.3 (C-2), 163.6 (C-4). MS-ESI *m/z* 209 (M$^+$, 100%). MS-AP *m/z* 209 (M$^+$, 100%). Anal. ($C_8H_{10}N_5O_4$) C, H, N.

6-[(4′-Aminoimidazol-1′-yl)methyl]-5-chlorouracil hydrochloride (4, X = Cl) was prepared as described for **4, X = H** using 5-chloro-6-[(4′-nitroimidazol-1′-yl)methyl]uracil (0.22 g, 0.8 mmol, 1 equiv), to give **4, X = Cl** as a beige powder (0.10 g, 44%). Mp >300 °C. ^{1}H NMR (DMSO-d_6): δ_H 5.07 (2H, s, CH_2), 6.96 (1H, d, $^4J_{HH}$ = 1.2 Hz, C5′-H), 7.14 (1H, d, $^4J_{HH}$ = 1.2 Hz, C2′-H), 8.16 (2H, s, $-NH_2$), 11.71 (1H, s, NH), 11.76 (1H, s, NH), 12.28 (1H, s, NH). ^{13}C NMR (DMSO-d_6): δ_C 43.5 (CH_2), 106.4 (C-5), 123.4 (C-4′), 125.4 (C-5′), 142.2 (C-2′), 144.6 (C-6), 149.7 (C-2), 159.6 (C-4). MS-ESI *m/z* 242 (^{35}Cl M$^+$, 100%), 244 (^{37}Cl M$^+$, 30%). Anal. ($C_8H_9Cl_2N_5O_2$) C, H, N.

6-[(4′-Aminoimidazol-1′-yl)methyl]-5-bromouracil hydrochloride (4, X = Br) was prepared as described for **4, X = H** using 5-bromo-6-[(4′-nitroimidazol-1′-yl)methyl]uracil (0.25 g, 0.8 mmol, 1 equiv), to give **4, X = Br** as a beige powder (0.10 g, 39%). Mp 267−268 °C. ^{1}H NMR (DMSO-d_6): δ_H 5.00 (2H, s, CH_2), 6.97 (1H, d, $^4J_{HH}$ = 1.2 Hz, C5′-H), 7.14 (1H, d, $^4J_{HH}$ = 1.2 Hz, C2′-H), 8.15 (2H, s, $-NH_2$), 11.68 (1H, s, NH), 11.72 (1H, s, NH) 12.25 (1H, s, NH). ^{13}C NMR (DMSO-d_6): δ_C 45.6 (CH_2), 96.9 (C-5), 123.4 (C-4′), 125.3 (C-5′), 142.2 (C-2′), 146.2 (C-6), 150.1 (C-2), 159.8 (C-4). MS-ESI *m/z* 286 (^{79}Br M$^+$, 100%), 288 (^{81}Br M$^+$, 95%). MS-AP *m/z* 286 (^{79}Br M$^+$, 100%), 288 (^{81}Br M$^+$, 96%). Anal. ($C_8H_9BrClN_5O_2$) C, H, N.

Assay of Substrates with TP. Assays for *E. coli* TP were conducted at 355 nm, 25 °C in 0.2 mL total volume containing 0.13 mM 5-nitro-2′-deoxyuridine, 0.1 M potassium phosphate (pH 7.4), and limiting amounts of TP (ca..0.00883 units per assay). Reaction was initiated by addition of TP. 5-Nitro-2′-deoxyuridine had a molar absorptivity coefficient of ϵ_M = 13300 M^{-1} cm^{-1} in 0.1 M phosphate buffer, pH 7.40 at 25 °C (literature values[51] pH 1 at 239 nm ϵ_M = 8050 M^{-1} cm^{-1} and at 304 nm ϵ_M = 10070 M^{-1} cm^{-1}, pH 12 at 321 nm ϵ_M = 14140 M^{-1} cm^{-1}). The conversion of 5-nitro-2′-deoxyuridine to 5-nitrouracil shows clear isosbestic points at λ = 325, 272, and 248 nm. The maximal absorbance changes occur in the region of ≥350 nm and a wavelength of 355 nm was chosen for the assay.

IC_{50} Values for Inhibitors with TP. The TP inhibition assay was carried out using the continuous spectrophotometric assay adapted for a 96-well plate instrument at 355 nm with 5-nitro-2′-deoxyuridine. To determine IC_{50} values, a 200 μL assay was carried out at a fixed saturated concentration of 5-nitro-2′-deoxyuridine (0.13 mM), and a fixed concentration of enzyme (45 nM) in a phosphate buffer (0.1 M, pH 7.4). Initial inhibitor stocks were prepared as 2−8 mM. If greater than 50% inhibition was obtained with 50 μL of this stock (0.5−2 mM final cuvette concentration), the initial stock was serially diluted in 10-fold stages until a suitable inhibition level was achieved. If no inhibition occurred at 1 mM the compound was considered not to be an inhibitor. For IC_{50} value estimation, 5−7 inhibitor concentrations were used spanning the IC_{50} value used. The initial velocity was plotted against inhibitor concentration and the IC_{50} value determined as the concentration causing a 50% decrease in the initial velocity relative to the mean of 2 or 3 controls with no inhibitor present, but the same amount of organic cosolvent (if any) used for the inhibitor studies. For inhibitors that were insoluble in aqueous media, stock solutions were made up in DMSO. The concentration of DMSO in the enzyme assay cuvette was never more than 0.5%, and this concentration was shown to have no effect on the kinetic data obtained.

***K_i* Values for Inhibitors with TP.** Experiments were conducted on selected compounds to determine the inhibition type and to measure their K_i values. To determine inhibition type and K_i values, initial rate assays were performed with four to six inhibitor concentrations chosen from an estimated determination of IC_{50} value and four or five different substrate concentrations (0.11, 0.22, 0.33, 0.43, 0.87 mM). The phosphate concentration was fixed and saturating (0.1 M). Inhibition type was diagnosed by reviewing the plotting patterns of plots of 1/*v* versus 1/[S] at various [I]; 1/*v* versus [I] at various [S], and [S]/*v* versus [I].

Aerobic and Anerobic Nitroreduction by XO. The kinetic constants (K_m and V_{max}), were determined from a continuous spectrophotometric assay, at 25 °C. The reaction mixtures (3.0 mL) contained 50 mM potassium phosphate buffer (pH 7.5), 0.15 mM xanthine solution (pH 7.5), and the prodrug substrates **3** and **4** in five different concentrations (25−150 μM). The reaction was initiated by injection of XO (0.9 U/mL). In the aerobic XO assays the cuvette was open to the atmosphere. In the anaerobic assay all solutions were degassed for 10 min, then gassed for 10 min with N_2 prior to incubation, and the reaction was monitored in a Hellma sealable quartz cuvette. The rate of the nitroreduction reaction was determined by continuous spectrophotometric monitoring of the decrease in extinction at 325 nm, the absorption maximum of the nitro chromophore.

Modeling TP Inhibitors with Human TP. The crystallographic coordinates for the 2.1 Å structure of human TP bound to the potent inhibitor TPI was obtained from AstraZeneca (PDB code: 1UOU).[25] Glu225 was modeled in non-ionized form due to very tight contacts with the carboxylate group of Asp114; in conjunction with changing histidine tautomeric forms, polar side chain conformations and waters were arranged to generate hydrogen bonding networks wherever possible; two unresolved residues, Glu238 and Ala239, were added.

The structure lacks the dianionic mono-hydrogen phosphate, essential for binding calculations of zwitterionic compounds, where electrostatics might be expected to dominate. To locate the binding mode of the phosphate within the closed TP structure, a transition-state complex was postulated within the active site, based on the orientation of the inhibitor and using initial 2′-deoxyribose C1′···O(P) and C1′···N1 distances of 2.1 and 2.2 Å, respectively. The waters and side-chains of active site residues were remodeled accordingly. Energy refinement of models having alternative conformations of the side chains of active-site cations Lys222 and Lys115, in combination with variations of the C1′···O(P) and C1′···N1 distances, led to a clear preference for a very open complex of the oxa-carbenium type. The well-defined orientations of the sugar and mono-hydrogen phosphate are part of a highly structured active site. The phosphate receives hydrogen bonds from Ser126OH, Ser144OH, Ser117NH, two from Lys115NH_3^+ and five from four waters, making 10 hydrogen bonds in total; the P−OH donates a hydrogen bond to Thr154Oγ. Waters in the highly-organized active site are involved in a minimum of three hydrogen bonds or energetic equivalents.

Based on the TP model including the phosphate, zwitterionic aminoimidazoyluracil inhibitors (**3**), and TPI and its bromo and nonhalogenated analogues, inhibitors were constructed in

the active site, with reoptimization of water networks. The uracil moieties of the inhibitors were modeled as the 2-oxyanion-3,4-dihydro-4-oxopyrimidine. Energy refinement of the complex was performed using the MMFF94s force field,[52] in conjunction with a dielectric constant of 1.3 within the Sybyl modeling package.[53] Following minimization of the TP−inhibitor complex, binding energies, E_{bind}, were determined as follows:

$$E_{bind} = E_{int} - \Delta G_{solv} \quad (1)$$

where $E_{int} = E_{RL} - (E_R + E_L)$. This interaction energy includes resolvation of the ligand by explicit water molecules at the active site. E_{bind} is corrected by an estimate of the ligand desolvation penalty, ΔG_{solv}, provided by the COSMO continuum solvent model[47,48] at the B3LYP/6-31+G* level of theory[54,55] averaged over three generated ligand solution conformations. These conformations contribute to the total energy of the unbound ligand (E_L). Electronic structure calculations were performed with the program Gaussian 98.[56]

Acknowledgment. This work was part-funded by the BBSRC, AICR, MRC, and Libyan Government. We would like to thank Dr. Richard Norman and Dr. Richard Pauptit for supplying us with the crystallographic coordinates for human TP, prior to publication, and Dr. Edwin Chinje for initial help with the XO assay.

Supporting Information Available: Elemental analysis data and Table S1 (absolute interaction and binding energies). This material is available free of charge via the Internet at http://pubs.acs.org.

References

(1) For a review see: Folkman, J. What is the role of thymidine phosphorylase in tumor angiogenesis? *J. Nat. Cancer. Inst.* **1996**, *88*, 1091−1092.
(2) For a review see: Griffiths, L.; Stratford, I. J. Platelet-derived endothelial cell growth factor thymidine phosphorylase in tumour growth and response to therapy. *Br. J. Cancer* **1997**, *76*, 689−693.
(3) For a review see: Cole, C.; Foster, A. J.; Freeman, S.; Jaffar, M.; Murray, P. E.; Stratford, I. J. The role of thymidine phosphorylase/PD-ECGF in cancer chemotherapy: a chemical perspective. *Anti-Cancer Drug Des.* **1999**, *14*, 383−392.
(4) For a review see: Focher, F.; Spadari, S. Thymidine phosphorylase: A two-face janus in anticancer chemotherapy. *Curr. Cancer Drug Targets* **2001**, *1*, 141−153.
(5) Birck, M. R.; Schramm, V. L. Nucleophilic participation in the transition state for human thymidine phosphorylase. *J. Am. Chem. Soc.* **2004**, *126*, 2447−2453.
(6) Brown, N. S.; Bicknell, R. Thymidine phosphorylase, 2-deoxy-D-ribose and angiogenesis. *Biochem. J.* **1998**, *334,* 1−8.
(7) Maeda, K.; Kang, S. M.; Ogawa, M.; Sawada, T.; Nakata, B.; Kato, Y.; Chung, Y. S.; Sowa, M. Combined analysis of vascular endothelial growth factor and platelet-derived endothelial cell growth factor expression in gastric carcinoma. *Int. J. Cancer* **1997**, *74*, 545−550.
(8) Takebayashi, Y.; Natsugoe, S.; Baba, M.; Akiba, S.; Fukumoto, T.; Miyadera, K.; Yamada, Y.; Takao, S.; Akiyama, S.; Aikou, T. Thymidine phosphorylase in human esophageal squamous cell carcinoma. *Cancer* **1999**, *85*, 282−289.
(9) Weidner, N.; Semple, J. P.; Welch, W. R.; Folkman, J. Tumor angiogenesis and metastasis-correlation in invasive breast carcinoma. *New Engl. J. Med*. **1991**, *324*, 1−8.
(10) Reynolds, K.; Farzaneh, F.; Collins, W. P.; Campbell, S.; Bourne, T. H.; Lawton, F.; Moghaddam, A.; Harris, A. L.; Bicknell, R. Association of ovarian malignancy with expression of platelet-derived endothelial cell growth factor. *J. Natl. Cancer Inst.* **1994**, *86*, 1234−1238.
(11) Relf, M.; LeJeune, S.; Scott, P. A.; Fox, S.; Smith, K.; Leek, R.; Moghaddam, A.; Whitehouse, R.; Bicknell, R.; Harris, A. L. Expression of the angiogenic factors vascular endothelial cell growth factor, acidic and basic fibroblast growth factor, tumor growth factor beta-1, platelet-derived endothelial cell growth factor, placenta growth factor, and pleiotrophin in human primary breast cancer and its relation to angiogenesis. *Cancer Res.* **1997**, *57*, 963−969.
(12) Kitazono, M.; Takebayashi, Y.; Ishitsuka, K.; Takao, S.; Tani, A.; Furukawa, T.; Miyadera, K.; Yamada, Y.; Aikou, T.; Akiyama, S. Prevention of hypoxia -induced apoptosis by the angiogenic factor thymidine phosphorylase. *Biochem. Biophys. Res. Commun.* **1998**, *253*, 797−803.
(13) Langen, P.; Etzold, G.; Barwolff, D.; Preussel, B. Inhibition of thymidine phosphorylase by 6-aminothymine and derivatives of 6-aminouracil. *Biochem. Pharmacol.* **1967**, *16*, 1833−1837.
(14) Pan, B. C.; Chen, Z. H.; Chu, E.; Chu, M. Y. W.; Chu, S. H. Synthesis of 5-halogeno-6-amino-2′-deoxyuridines and their analogues as potential inhibitors of thymidine phosphorylase. *Nucleosides Nucleotides* **1998**, *17*, 2367−2382.
(15) Haraguchi, M.; Miyadera, K.; Uemura, K.; Sumizawa, T.; Furukawa, T.; Yamada, K.; Akiyama, S.; Yamada, Y. Angiogenic activity of enzymes. *Nature* **1994**, *368*, 198.
(16) Balzarini, J.; Gamboa, A. E.; Esnouf, R.; Liekens, S.; Neyts, J.; de Clercq, E.; Camarasa, M.-J.; Perez-Perez, M. J. 7-Deazaxanthine, a novel prototype inhibitor of thymidine phosphorylase. *FEBS Lett.* **1998**, *438*, 91−95.
(17) Yano, S.; Tada, Y.; Kuzuno, H.; Suto, T.; Tamashita, J.; Suzuki, N.; Emura, T.; Fukushima, M.; Asao, T. Int. Patent Appl. WO 96/30346, 1996.
(18) Suzuki, N.; Fukushima, M.; Asao, T.; Yamada, Y.; Akiyama, S. Invention of a novel antitumour agent, TAS-102. (2) Antitumor activities of 5-trifluorothymidine combined with a new inhibitor of thymidine phosphorylase. *Proc. Am. Assoc. Cancer Res.* **1997**, *38*, 101.
(19) Matsushita, S.; Nitanda, T.; Furukawa, T.; Sumizawa, T.; Tani, A.; Nishimoto, K.; Akiba, S.; Miyadera, K.; Fukushima, M.; Yamada, Y.; Yoshida, H.; Kanzaki, T.; Akiyama, S. The effect of a thymidine phosphorylase inhibitor on angiogenesis and apoptosis in tumors. *Cancer Res.* **1999**, *59*, 1911−1916.
(20) Yano, S.; Kazuno, H.; Sato, T.; Suzuki, N.; Emura, T.; Wierzba, K.; Yamashita, J.; Tada, Y.; Yamada, Y.; Fukushima, M.; Asao, T. Synthesis and evaluation of 6-methylene-bridged uracil derivatives. Part 2: Optimization of inhibitors of human thymidine phosphorylase and their selectivity with uridine phosphorylase. *Bioorg. Med. Chem.* **2004**, *12*, 3443−3450.
(21) A preliminary account of this work has been published: Cole, C.; Reigan, P.; Gbaj, A.; Edwards, P. N.; Douglas, K. T.; Stratford, I. J.; Freeman, S.; Jaffar, M. Potential tumor-selective nitroimidazolylmethyluracil prodrug derivatives: Inhibitors of the angiogenic enzyme thymidine phosphorylase. *J. Med. Chem.* **2003**, *46*, 207−209.
(22) Cole, C.; Marks, D. S.; Jaffar, M.; Stratford, I. J.; Douglas, K. T.; Freeman, S. A similarity model for the human angiogenic factor, thymidine phosphorylase/platelet derived-endothelial cell growth factor. *Anti-Cancer Drug Des.* **1999**, *14*, 411−420.
(23) Walter, M. R.; Cook, W. J.; Cole, L. B.; Short, S. A.; Koszalka, G. W.; Krenitsky, T. A.; Ealick, S. E. Three-dimensional structure of thymidine phosphorylase from *Escherichia coli* at 2.8 A resolution. *J. Biol. Chem.* **1990**, *265*, 14016−14022.
(24) Ishikawa, F.; Miyazono, K.; Hellman, U.; Drexler, H.; Wernstedt, C.; Hagiwara, K.; Usuki, K.; Takaku, F.; Risau, W.; Heldin, C. H. Identification of angiogenic activity and the cloning and expression of platelet-derived endothelial cell growth factor. *Nature* **1989**, *338*, 557−562.
(25) Norman, R. A.; Barry, S. T.; Bate, M.; Breed, J.; Colls, J. G.; Ernill, R. J.; Luke, R. W. A.; Minshull, C. A.; McAlister, M. S. B.; McCall, E. J.; McMiken, H. H. J.; Paterson, D. S.; Timms, D.; Tucker, J. A.; Pauptit, R. A. Crystal structure of human thymidine phosphorylase in complex with a small molecule inhibitor. *Structure* **2004**, *12*, 75−84.
(26) Murray, P. E.; McNally, V. A.; Lockyer, S. D.; Williams, K. J., Stratford, I. J.; Jaffar, M.; Freeman, S. Synthesis and enzymatic evaluation of pyridinium-substituted uracil derivatives as novel inhibitors of thymidine phosphorylase. *Bioorg. Med. Chem.* **2002**, *10*, 525−530.
(27) Yano, S.; Kazuno, H.; Suzuki, N.; Emura, T.; Wierzba, K.; Yamashita, J.; Tada, Y.; Yamada, Y.; Fukushima, M.; Asao, T. Synthesis and evaluation of 6-methylene-bridged uracil derivatives. Part 1: Discovery of novel orally active inhibitors of human thymidine phosphorylase. *Bioorg. Med. Chem.* **2004**, *12*, 3431−3441.
(28) Wataya, Y.; Santi, D. W. Continuous spectrophotometric assay of thymidine phosphorylase using 5-nitro-2′-deoxyuridine as substrate. *Anal. Biochem.* **1981**, *112*, 96−98.
(29) Schwartz, M. Thymidine phosphorylase from *Escherichia coli*. Properties and kinetics. *Eur. J. Biochem*. **1971**, *21*, 191−198.
(30) Nakayama, C.; Wataya, Y.; Meyer, R. B., Jr.; Santi, D. V.; Saneyoshi, M.; Ueda, T. Thymidine phosphorylase. Substrate specificity for 5-substituted 2′-deoxyuridines. *J. Med. Chem*. **1980**, *23*, 962−964.
(31) Esteban-Gamboa, A.; Balzarini, J.; Esnouf, R.; De Clercq, E.; Camarasa, M. J.; Perez-Perez, M. J. Design, synthesis, and enzymatic evaluation of multisubstrate analogue inhibitors of *Escherichia coli* thymidine phosphorylase. *J. Med. Chem*. **2000**, *43*, 971−983.

(32) Klein, R. S.; Lenzi, M.; Lim, T. H.; Hotchkiss, K. A.; Wilson, P.; Schwartz, E. L. Novel 6-substituted uracil analogues as inhibitors of the angiogenic actions of thymidine phosphorylase. *Biochem. Pharmacol*. **2001**, *62*, 1257−1263.
(33) Balzarini, J.; Degreve, B.; Esteban-Gamboa, A.; Esnouf, R.; De Clercq, E.; Engelborghs, Y.; Camarasa, M. J.; Perez-Perez, M. J. Kinetic analysis of novel multisubstrate analogue inhibitors of thymidine phosphorylase. *FEBS Lett.* **2000**, *483*, 181−185.
(34) Gbaj, A.; MPhil thesis, University of Manchester, 2003.
(35) Jenkins, T. C.; Naylor, M. A.; O'Neill, P.; Threadgill, M. D.; Cole, S.; Stratford, I. J.; Adams, G. E.; Fielden, E. M.; Suto, M. J.; Stier, M. A. Synthesis and evaluation of alpha-[[(2-haloethyl)-amino]methyl]-2-nitro-1*H*-imidazole-1-ethanols as prodrugs of alpha-[(1-aziridinyl)methyl]-2-nitro-1*H*-imidazole-1-ethanol (RSU-1069) and its analogues which are radiosensitizers and bioreductively activated cytotoxins. *J. Med. Chem.* **1990**, *33*, 2603−2610.
(36) Naylor, M. A.; Threadgill, M. D.; Webb, P.; Stratford, I. J.; Stephens, M. A.; Fielden, E. M.; Adams, G. E. 2-Nitroimidazole dual-function bioreductive drugs − studies on the effects of regioisomerism and side-chain structural modifications on differential cytotoxicity and radiosensitization by aziridinyl and oxiranyl derivatives. *J. Med. Chem.* **1992**, *35*, 3573−3578.
(37) Hay, M. P.; Wilson, W. R.; Denny, W. A. Design, synthesis and evaluation of imidazolylmethyl carbamate prodrugs of alkylating agents. *Tetrahedron* **2000**, *56*, 645−657.
(38) Clarke, E. D.; Goulding, K. H.; Wardman, P. Nitroimidazoles as anaerobic electron acceptors for xanthine oxidase. *Biochem. Pharmacol.* **1982**, *31*, 3237−42.
(39) Clarke, E. D.; Wardman, P.; Goulding, K. H. Anaerobic reduction of nitroimidazoles by reduced flavin mononucleotide and by xanthine oxidase. *Biochem. Pharmacol.* **1980**, *29*, 2684−7.
(40) Tatsumi, K.; Kitamura, S.; Yoshimura, H.; Kawazoe, Y. Susceptibility of aromatic nitro compounds to xanthine oxidase-catalyzed reduction. *Chem. Pharm. Bull. (Tokyo)* **1978**, *26*, 1713−7.
(41) Walton, M. I.; Workman, P. Nitroimidazole bioreductive metabolism. Quantitation and characterisation of mouse tissue benznidazole nitroreductases in vivo and in vitro. *Biochem. Pharmacol.* **1987**, *36*, 887−896.
(42) Anderson, R. F.; Patel, K. B.; Reghebi, K.; Hill, S. A. Conversion of xanthine dehydrogenase to xanthine oxidase as a positive marker for hypoxia in tumours and normal tissues. *Br. J. Cancer* **1989**, *60*, 193−197.
(43) Bolton, J. L.; McClelland, R. A. Kinetics and mechanism of the decomposition in aqueous solutions of 2-(hydroxyamino)imidazoles. *J. Am. Chem. Soc.* **1989**, *111*, 8172−8181.
(44) Topol, I. A.; Tawa, G. J.; Burt, S. K.; Rashin, A. A. Calculation of absolute and relative acidities of substituted imidazoles in aqueous solvent. *J. Phys. Chem. A* **1997**, *101*, 10075−10081.
(45) Robison, M. M.; Butler, F. P.; Robison, B. L. 7-Azaindole. IV. The hydrogenation of 7-azaindole and related compounds. *J. Am. Chem. Soc*. **1957**, *79*, 2573−2577.
(46) Levene, P. A.; Bass, L. W.; Simms, H. S. Ionization of pyrimidines in relation to the structure of pyrimidine nucleosides. *J. Biol. Chem*. **1926**, *70*, 229−241.
(47) Klamt, A.; Schüürmann, G. COSMO − A new approach to dielectric screening in solvents with explicit expressions for the screening energy and its gradient. *J. Chem. Soc., Perkin Trans.* **1993**, *2*, 799−805.
(48) Barone, V.; Cossi, M. Quantum calculation of molecular energies and energy gradients in solution by a conductor solvent model. *J. Phys. Chem.* **1998**, *102*, 1995−2001.
(49) Gallo, G. G.; Pasqualucci, C. R.; Radaelli, P.; Lancini, G. C.; The Ionization Constants of Some Imidazoles. *J. Org. Chem.* **1964**, *29*, 862−865.
(50) Giziewicz, J.; Wnuk, S. F.; Robins, M. J. Nucleic acid related compounds. 107. Efficient nitration of uracil base and nucleoside derivatives. *J. Org. Chem*. **1999**, *64*, 2149−2151.
(51) Huang, G. F.; Torrence, P. F. Nitration of pyrimidine bases and nucleotides by nitronium tetrafluoroborate. *J. Org. Chem*. **1977**, *42*, 3821−3824.
(52) Halgren T. A. MMFF VI. MMFF94s option for energy minimization studies. *J. Comput. Chem.* **1999**, *20*, 720−729.
(53) SYBYL 6.8, Tripos Inc., St. Louis, MO, 2003.
(54) Becke, A. D. Density-functional thermochemistry. 3. The role of exact exchange. *J. Chem. Phys.* **1993**, *98*, 5648−5652.
(55) Hehre, W. J.; Ditchfield, R.; Pople, J. A. Self-consistent molecular orbital methods. 12. Further extension of Gaussian-type basis sets for use in molecular-orbital studies of organic molecules. *J. Chem. Phys.* **1972**, *56*, 2257−2261.
(56) Frisch, M. J.; Trucks, G. W.; Schlegel, H. B.; Scuseria, G. E.; Robb, M. A.; Cheeseman, J. R.; Zakrzewski, V. G.; Montgomery, J. A.; Stratmann, R. E.; Burant, J. C.; Dapprich, S.; Millam, J. M.; Daniels, A. D.; Kudin, K. N.; Strain, M. C.; Farkas, O.; Tomasi, J.; Barone, V.; Cossi, M.; Cammi, R.; Menucci, B.; Pomelli, C.; Adamo, C.; Clifford, S.; Ochterski, J.; Petersson, G. A.; Ayala, P. Y.; Cui, Q.; Morokuma, K.; Malick, D. K.; Rabuck, A. D.; Raghavachari, K.; Foresman, J. B.; Cioslowski, J.; Ortiz, J. V.; Stefanov, B. B.; Liu, G.; Liashenko, A.; Piskorz, P.; Komaromi, I.; Gomperts, R.; Martin, R. L.; Fox, D. J.; Keith, T. A.; Al-Laham, M. A.; Peng, C. Y.; Nanayakkara, A.; Gonzalez, C.; Challacombe, M.; Gill, P. M. W.; Johnson, B. G.; Chen, W.; Wong, M. W.; Andres, J. L.; Head-Gordon, M.; Replogle, E. S.; Pople, J. A. GAUSSIAN98, Revision A.1; Pittsburgh, PA, 1998.

JM049494R